Keon, J. P. R., Antoniw, J. F., Carzaniga, R., Deller, S., Ward, J. L., Baker, J. M., Beale, M. H., Hammond-Kosack, K. E. and Rudd, J. J. 2007. Transcriptional adaptation of Mycosphaerella graminicola to programmed cell death (PCD) of its susceptible wheat host. *Molecular Plant-Microbe Interactions.* 20 (2), pp. 178-193.

MPMI Vol. 20, No. 2, 2007, pp. 178–193. DOI: 10.1094/MPMI-20-2-0178. *e*-Xtra*

Transcriptional Adaptation of *Mycosphaerella graminicola* to Programmed Cell Death (PCD) of Its Susceptible Wheat Host

John Keon,[1] John Antoniw,[1] Raffaella Carzaniga,[2] Siân Deller,[1] Jane L. Ward,[3] John M. Baker,[3] Michael H. Beale,[3] Kim Hammond-Kosack,[1] and Jason J. Rudd[1]

[1]Wheat Pathogenesis Programme, Plant-Pathogen Interactions Division, Rothamsted Research, Harpenden, Herts AL5 2JQ, U.K.; [2]Current address- Centre for Molecular Microbiology and Infection, Department of Infectious Diseases, South Kensington Campus Imperial College London, London. SW7 2AZ, U.K.; [3]National Centre for Plant and Microbial Metabolomics, Rothamsted Research, West Common, Harpenden, Herts. AL5 2JQ, U.K.

Submitted 14 July 2006. Accepted 16 August 2006.

Many important fungal pathogens of plants spend long periods (days to weeks) of their infection cycle in symptomless association with living host tissue, followed by a sudden transition to necrotrophic feeding as host tissue death occurs. Little is known about either the host responses associated with this sudden transition or the specific adaptations made by the pathogen to invoke or tolerate it. We are studying a major host-specific fungal pathogen of cultivated wheat, *Septoria tritici* (teleomorph *Mycosphaerella graminicola*). Here, we describe the host responses of wheat leaves infected with *M. graminicola* during the development of disease symptoms and use microarray transcription profiling to identify adaptive responses of the fungus to its changing environment. We show that symptom development on a susceptible host genotype has features reminiscent of the hypersensitive response, a rapid and strictly localized form of host programmed cell death (PCD) more commonly associated with disease-resistance mechanisms. The initiation and advancement of this host response is associated with a loss of cell-membrane integrity and dramatic increases in apoplastic metabolites and the rate of fungal growth. Microarray analysis of the fungal genes differentially expressed before and after the onset of host PCD supports a transition to more rapid growth. Specific physiological adaptation of the fungus is also revealed with respect to membrane transport, chemical and oxidative stress mechanisms, and metabolism. Our data support the hypothesis that host plant PCD plays an important role in susceptibility towards fungal pathogens with necrotrophic lifestyles.

Additional keywords: cytochrome c release, DNA fragmentation, ^{1}H-NMR, *Mycosphaerella fijiensis*, pycnidia, reactive oxygen species.

Fungal pathogenesis of plants can be classified into three general categories based upon the mode of nutrition during the interaction with the host (Oliver and Ipcho 2004; Thrower 1966). Necrotrophic fungi are characterized as feeding exclusively on dead or dying host tissue, which is triggered rapidly by the pathogen following the onset of the interaction. In contrast, biotrophic fungi require living host tissue to supply their nutrients and are often controlled by a form of host programmed cell death (PCD) referred to as the hypersensitive response (HR). In between these two extremes are hemibiotrophic pathogens, which are suggested to spend a significant proportion of their infection cycle feeding as biotrophs before suddenly switching to necrotrophy as host tissue collapses (Luttrell 1974).

We are studying a major host-specific fungal pathogen of cultivated wheat (*Triticum aestivum*), *Mycosphaerella graminicola*, the causal agent of septoria leaf blotch disease, one of the most devastating diseases affecting global grain production (Eyal 1999). Infection of wheat leaves by *M. graminicola* is associated with a long delay (latent period) before the appearance of the first visible symptoms of disease, which can extend to several weeks after inoculation. For these reasons *M. graminicola* and related species have often been referred to as hemibiotrophic, based on the assumption that the symptomless-growth phase involves the fungus successfully acquiring sufficient nutrients from living tissue and, thus, initially feeding biotrophically (Luttrell 1974; Parbery 1996). Five distinct phases have been described for the infection cycle of *M. graminicola* (Kema et al. 1996). Leaf penetration occurs via stomata within 3 days of inoculation. The fungus then lives asymptomatically for up to 10 to 14 days, during which time it begins to colonize substomatal cavities and the apoplast surrounding leaf mesophyll cells. Necrotrophic feeding begins as disease symptoms appear (host-tissue collapse) and, from this point on, growth of the fungus becomes more rapid. This phase also involves the development of asexual sporulation structures, pycnidia, below stomata, from which the fungus re-emerges in the form of pycnidiospores awaiting rain-splash propagation to other leaves of the plant. Importantly and in contrast to many other fungal pathogens of plants, *M. graminicola* is not known to develop any specialized penetration or feeding structures and remains apoplastic throughout the entire infection cycle (Kema et al. 1996).

Disease symptoms on infected leaves of susceptible wheat plants manifest themselves in the abrupt appearance of chlorotic and necrotic lesions within which the fungus ultimately sporulates. It has been suggested that these symptoms may be triggered by the fungus via the production of some form of toxin (Kema et al. 1996), although to date no such

Corresponding author: J. J. Rudd; E-mail: jason.rudd@bbsrc.ac.uk; Fax: +44(0) 1582 760981.

*The *e*-Xtra logo stands for "electronic extra" and indicates the HTML abstract available on-line contains supplemental material not included in the print edition. A supplementary figure and two tables appear on-line.

candidate agent has been identified. Many forms of plant cell death are now recognized as being orchestrated in a regulated manner by mechanisms that are referred to as PCD (Van Doorn and Woltering 2005). Several forms of PCD appear in plants, but the one most commonly associated with resistance responses to pathogens is the HR (Beers and McDowell 2001; Greenberg and Yao 2004; Heath 2000). This very rapid and strictly localized form of plant PCD is often a successful means by which plants prevent further development and spread of, in particular, biotrophic leaf pathogens and has recently been identified as an autophagic response (Liu et al. 2005). Many similarities have been identified between forms of plant cell death and apoptotic responses of animal cells, including changes in plasma membrane integrity, mitochondrial cytochrome c release, activation of cysteine proteases, and characteristic DNA laddering (Chichkova et al. 2004; Coffeen and Wolpert 2004; Curtis and Wolpert 2004; del Pozo and Lam 1998; Krause and Durner 2004; Navarre and Wolpert 1999b; Ryerson and Heath 1996; Woltering 2004). Other studies have also suggested HR-like cell death to be a feature of disease susceptibility when it may actually facilitate plant infection by necrotrophic fungal pathogens (Govrin and Levine 2000; Lincoln et al. 2002; Van Baarlen et al. 2004; Yao et al. 2002). The pathogens under investigation in these studies were often seen to trigger host cell-death responses within hours or days of first contact.

We have developed a *M. graminicola* cDNA microarray containing 2,563 unisequences that has been used to investigate changes in gene expression in response to different defined in vitro nutritional environments and at a very late stage of host plant infection, during which the fungus is sporulating profusely in fully necrotic leaves (Keon et al. 2005a and b). These studies identified the environment of the sporulating fungus to be nutrient-rich (Keon et al. 2005a and b). The genome of *Mycosphaerella graminicola* has recently been sequenced by the Joint Genome Institute of the United States Department of Energy, and first analysis suggests the presence of approximately 11,400 genes. Therefore, the microarray used in these studies is expected to contain between a quarter and a fifth of the total number of genes present.

The present study reports an investigation of the physiological changes in both host and pathogen during the sudden development of macroscopic disease symptoms. We have introduced adaptations to an established bioassay that has permitted a study of this phenomenon simultaneously from the point of view of both the pathogen and the host. By monitoring the expression of 2,563 *M. graminicola* genes during development of host cell-death symptoms in vivo, we provide important novel insights into the infection biology of this pathogen. Furthermore, we present evidence that symptom development and disease susceptibility share features of HR-like PCD. This study offers a first insight into the transcriptional changes of a successful host-specific plant pathogen as it overcomes this dramatic means of host defense and also questions the validity of referring to *M. graminicola* as a hemibiotrophic fungal pathogen.

RESULTS

Development of an in vivo bioassay for the simultaneous investigation of host and pathogen responses during the disease transition.

Preliminary experiments were first undertaken to identify the stages of fungal infection that represented both the immediate pre- and postdisease transitional states, based upon the first appearance of visible symptoms. To enable the transcription profiling of *M. graminicola* during these phases, we first performed a dose-response analysis using serial dilution of sporidia inoculated evenly onto 7-cm-long regions of attached wheat leaves. We then recorded symptom development at 13 and 21 days through to advanced pycnidial development in necrotic tissue (Fig. 1A). Serial dilution of the sporidia resulted in a more "patchy" appearance of symptoms over the inoculated area, being similar to that seen after natural infection in the field. Even at lower inoculum levels, the time taken to first appearance of pycnidia was unaffected, but they appeared within discrete lesions as opposed to being uniformly spread across the whole inoculated area at the higher densities (Fig. 1A). This result identified the requirement of using high inoculum levels in order to establish synchronous disease development across the inoculated regions. An inoculum of 1×10^7 sporidia per milliliter was used for all further experiments (corresponding to approximately 400,000 spores per leaf as shown in Figure 1A). We then selected our sampling timepoints by inoculating 4-cm-long regions of wheat leaves and monitoring symptom development on the same leaves on a daily basis. Figure 1B shows a typical result. First visible symptoms of disease were observed on day 9. Importantly, the symptoms developed uniformly across the entire inoculated area. From day 9 or 10 onwards, symptoms developed rapidly, giving rise to leaf necrosis and the formation of immature asexual sporulation structures (pycnidial initials) around days 14 to 15. It is noteworthy that initial symptoms developed only in the inoculated regions of the leaves, thus highlighting the strict localization of the response. We selected days 9, 10, and 14 for fungal microarray analysis.

Disease symptoms develop first as water-soaked lesions positively influenced by illumination.

Closer inspection of the first appearance of symptoms on inoculated leaves revealed that development of necrotic "speckles" was immediately preceded by small water-soaked regions that appeared suddenly the evening before (approximately 16 h). These water-soaked regions were replaced by necrotic tissue the following morning, and new water-soaked regions could then be seen once again in the late afternoon. Figure 2A displays this phenomenon for symptoms appearing on days 9 and 10 on an inoculated leaf. An additional feature of disease development was the first appearance of symptoms on the upper surfaces (light facing) of leaves irrespective of the surface to which the inoculum was applied (data not shown). This was true also for the subsequent development of pycnidia. This suggested that illumination influenced the appearance of disease symptoms. We performed some periodic shading experiments to further study this aspect. Figure 2B shows the effect of shading inoculated leaves from day 7 to 13 on the levels of symptoms observed at day 13 and then at day 17, when subsequently left unshaded. Figure 2B demonstrates that shading the inoculated leaves retarded the characteristic chlorosis and necrosis responses normally seen by day 13. However, when then left exposed to light until day 17, the shaded leaves rapidly underwent these responses, and pycnidia developed, albeit to a lesser extent than in the unshaded leaves. These observations suggest that the quality and direction of illumination play key roles in symptom development during the normal infection process of *M. graminicola*.

Levels of reactive oxygen species (ROS) increase as disease symptoms develop in infected leaves.

Cell death and defense responses of plants are often associated with changes in the production of ROS, including superoxide and hydrogen peroxide, which can be visualized by staining with nitroblue tetrazolium (NBT) and diaminobenzidine (DAB), respectively (Adam et al. 1989; Thordal-Christensen et

al. 1997). It has previously been shown that the absolute levels of H_2O_2 rise dramatically in *M. graminicola*–infected leaves during the onset of visible disease (Shetty et al. 2003); however, the origin and localization of these ROS remains unclear. We therefore investigated and compared the presence and localization of both superoxide and H_2O_2 in the day 10 and day 14 inoculated leaves (Fig. 2C) selected for fungal microarray analysis. At day 10, superoxide was detected in discrete regions corresponding to areas that appear as water-soaked at this timepoint. Hydrogen peroxide was detected diffusely throughout this material. On day 14 both superoxide and hydrogen peroxide were strongly associated with the developing pycnidial initials (Fig. 2C, appearing as intensely stained spots). We have previously shown that mature pycnidia in a fully necrotic leaf at a very late stage of infection also stain strongly for both superoxide and hydrogen peroxide, which suggested that they were produced by the fungus (Keon et al. 2005b). We investigated more closely the distribution of these ROS in the developing pycnidia via sectioning and light microscopy (Fig. 2D). These analyses demonstrated a large amount of hydrogen peroxide to be present surrounding the fungal structures in close association with the walls of the substomatal cavity. In contrast, superoxide was restricted to undefined vesicular structures present within the fungal material. To summarize, and as highlighted in Figure 2C, a dramatic overall increase in the levels of superoxide and hydrogen peroxide was visible in the inoculated tissue when comparing day 10 with day 14 tissues. However, it remains to be determined whether these ROS originate from the host or pathogen (or both) during this phase of the interaction.

Symptom development involves features of host PCD and correlates with an increase in fungal growth rate.

The visible symptoms described thus far suggest the triggering of a rapid host cell-death response as disease develops. We investigated the possibility that this was, in fact, a form of PCD by looking for characteristic physiological markers for this phenomenon. First, we investigated the localization of cytochrome c throughout the infection timecourse via Western blotting on leaf cytosolic and microsomal extracts (Fig. 3A). A

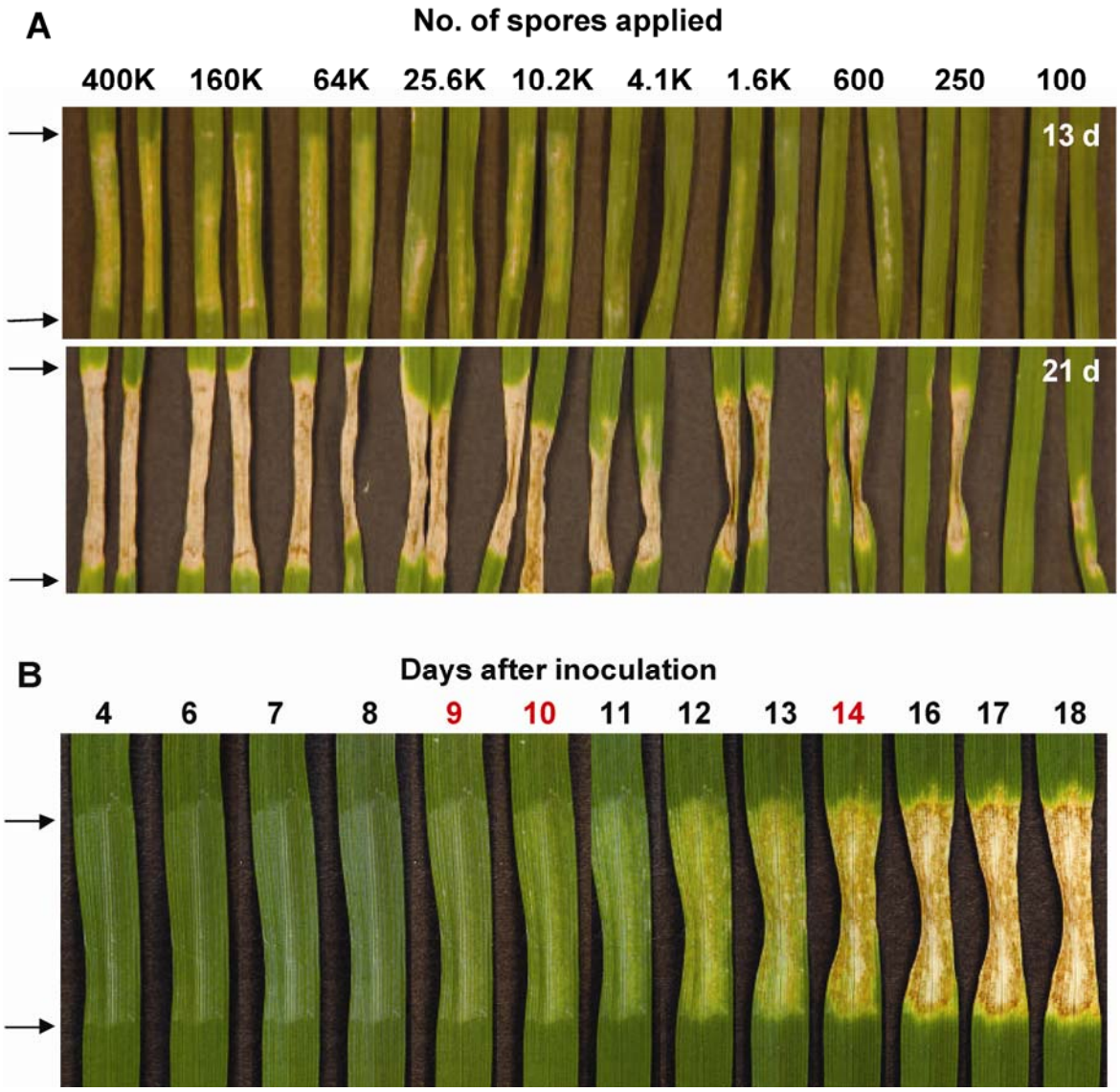

Fig. 1. Development of a bioassay for simultaneous investigation of fungal and host physiology during infection. **A,** Fungal sporidia were harvested from plates and applied in serial dilution (ranging from 400,000 [400K] to 100 spores) to wheat leaves in duplicate. Disease symptoms were assessed at both 13 and 21 days following inoculation. Arrows delimit the area inoculated. **B,** Timecourse for symptom development. A representative leaf was inoculated with approximately 400,000 fungal sporidia and was photographed at 24-h intervals. Note the high inoculum dose introduces a synchronous infection phenotype in the inoculated region that does not spread beyond this region. Leaf material represented by days 9 or 10 and 14 were taken for subsequent microarray analysis (labeled in red).

clear accumulation of cytochrome c in the cytosol was evident on day 10 and even more pronounced by day 14. Simultaneous analysis of the microsomal fraction failed to detect the presence of cytochrome c on day 14 strongly suggesting that the accumulation observed in the cytosol resulted from mitochondrial release (Fig. 3A). Cytochrome c release in animal cells typically triggers protease cascades leading to the characteristic internucleosomal cleavage of DNA visualized as laddering in agarose gels. We collected inoculated leaves from day 8 onwards and investigated the integrity of host genomic DNA. Figure 3B shows a typical result. This analysis identified a marked DNA laddering response (fragments differing by approximately 180 bp) initiated as disease symptoms developed in the inoculated leaves.

We then assayed for changes in membrane integrity by measuring electrolyte leakage into an ion-free bathing solution (deionized water). Leaf segments from inoculated plants were subjected to ion-leakage analysis at 24-h intervals from day 5 to day 13. The results of this analysis are shown in Figure 3C. The data confirmed that the visible symptoms appearing as water-soaked lesions on day 9 coincide with the onset of an increase in ion leakage from damaged cells. These results are consistent with a widespread and accelerating loss of membrane integrity typical of cell lysis, necrosis, and death. This response was restricted to the mesophyll cells, while the epidermal cells remained unaffected until very late stages of disease (data not shown). We simultaneously measured the level of fungal biomass in the leaf material over this period using real-time polymerase chain reaction (PCR) against genomic DNA (Fraaije et al. 2005). The fungal growth curve is plotted onto Figure 3C to allow comparison with the ion-leakage data and clearly demonstrates a sudden increase in measurable fungal biomass following the initiation and advancement of host membrane damage. The data also demonstrates that day 9 or 10 represents the onset of a measurable increase in fungal growth in this bioassay. The rapid deterioration of the host across the transition was also illustrated by the sudden disappearance of chloroplastic rRNA species by day 14 of

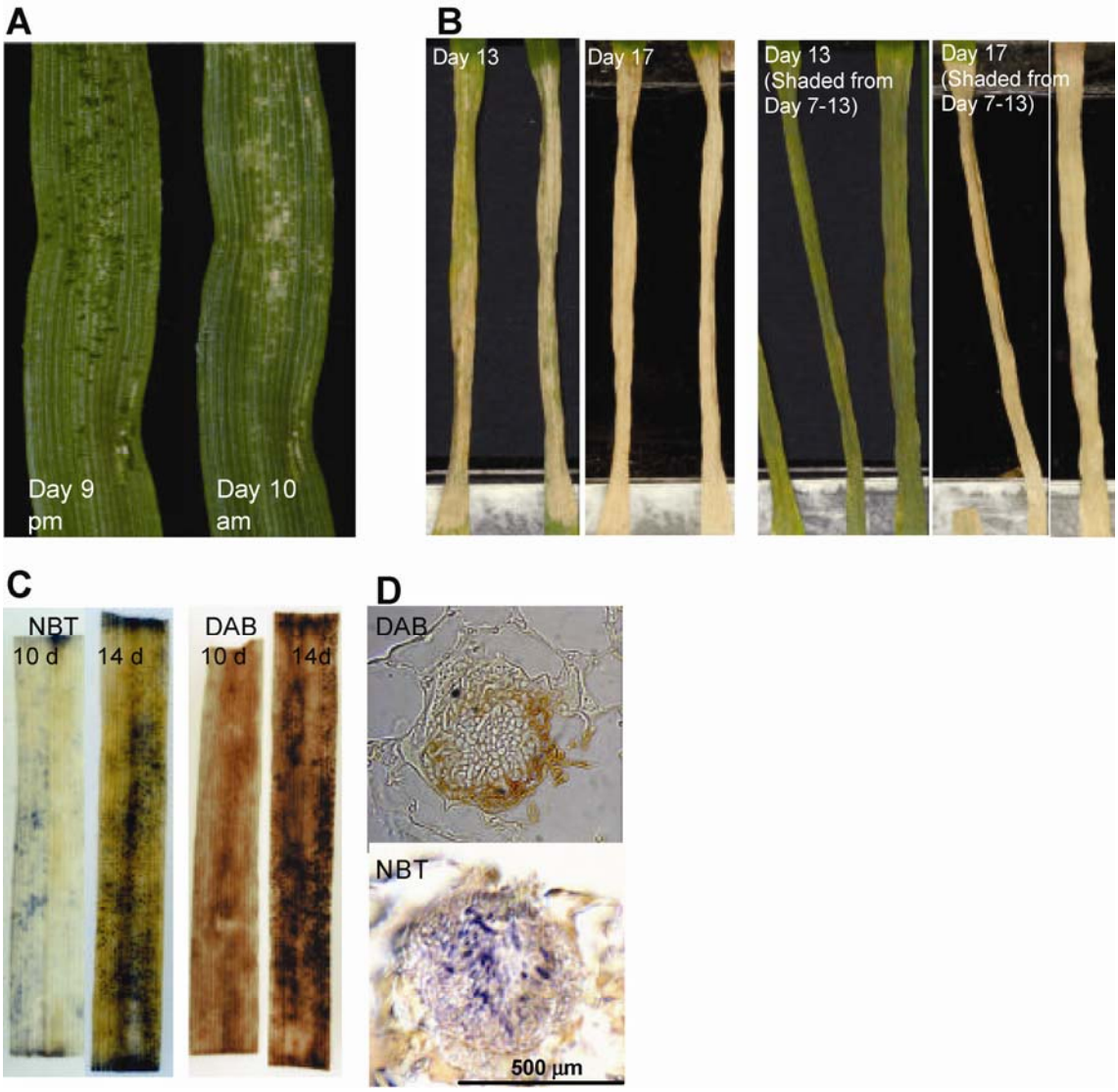

Fig. 2. Disease symptoms develop as water soaked lesions influenced by illumination and associated with increases in reactive oxygen species (ROS). **A,** Necrotic lesions on inoculated leaves are preceded (approximately 16 h) by water-soaked regions. **B,** Inoculated leaves were allowed to develop symptoms under full illumination or were shaded prior to the development of first symptoms (from days 7 to 13). Photographs were then taken. Shading inoculated leaves delays both the chlorosis and necrosis responses. **C,** Inoculated leaves (10 and 14 days) were stained for the ROS $O_2^{\cdot-}$ (nitroblue tetrazolium [NBT] stain—blue/violet) and H_2O_2 (diaminobenzidine [DAB] stain—red/brown). Overall levels of ROS in inoculated leaves increase from day 10 to day 14. **D,** Mature pycnidia stain strongly for $O_2^{\cdot-}$ and H_2O_2. Inoculated leaves (21 days) were stained with either NBT or DAB and were sectioned for light microscopy. $O_2^{\cdot-}$ is detected within fungal sporulation structures, whereas H_2O_2 surrounds the structures in the vicinity of the wall of the stomatal cavity.

infection (Fig. 3D, arrowed). These data collectively suggest disease symptom development involves the triggering of a sudden PCD response in the infected host tissue and suggests that a dramatic change in the environment surrounding the fungus occurs when advancing from day 9 or 10 to day 14 of infection.

Analysis of apoplastic amino acid and sugar content during phases of plant infection by *M. graminicola*.

As *Mycosphaerella graminicola* remains apoplastic throughout infection, we sought to determine whether the plant PCD response might be triggered as a consequence of the fungus depleting the apoplast surrounding the mesophyll cells of nutrients and, in particular, amino acids and sugars. To investigate this, day 6 (symptomless growth), day 9 (first onset of symptoms), and day 13 (advancing host PCD) inoculated or mock-inoculated (water without fungal sporidia) leaves were collected, and the apoplastic fluids were analyzed by ^{1}H-nuclear magnetic resonance (NMR). The traces for the identifiable amino acids and sugars are presented in Figure 4A for each condition. By comparing mock-inoculated profiles with the corresponding inoculated timepoint, it is clear that no major qualitative or quantitative differences are seen at day 6. This suggests that the fungus is not dramatically depleting the apoplast of metabolites during the symptomless-growth phase. Analysis of the day 9 material shows that the onset of host PCD results in the first minor but measurable increase in the apoplastic contents of all the identifiable metabolites. By day 13, it is clear that the advancing host PCD has resulted in a large increase in all the measurable metabolites in the apoplastic fluid. Importantly, we were unable to detect the fungal-specific metabolites trehalose or mannitol in any of the samples investigated, suggesting that the overall increases in apoplastic metabolites predominantly resulted from release from plant cells, although we cannot discard the possibility that small amounts of fungal metabolites may also be present. Thus, the loss of host-membrane integrity during the onset of PCD may serve to provide a large and diverse mixture of potential apoplastic nutrients to the fungus. Importantly, there was no evidence of the fungus depleting apoplastic nutrients during the symptomless phase of the interaction. Principle component analysis (PCA) of the full spectra (including three experimental replicates for each sample) was also performed, and the scores plot of the first two components is presented in Figure

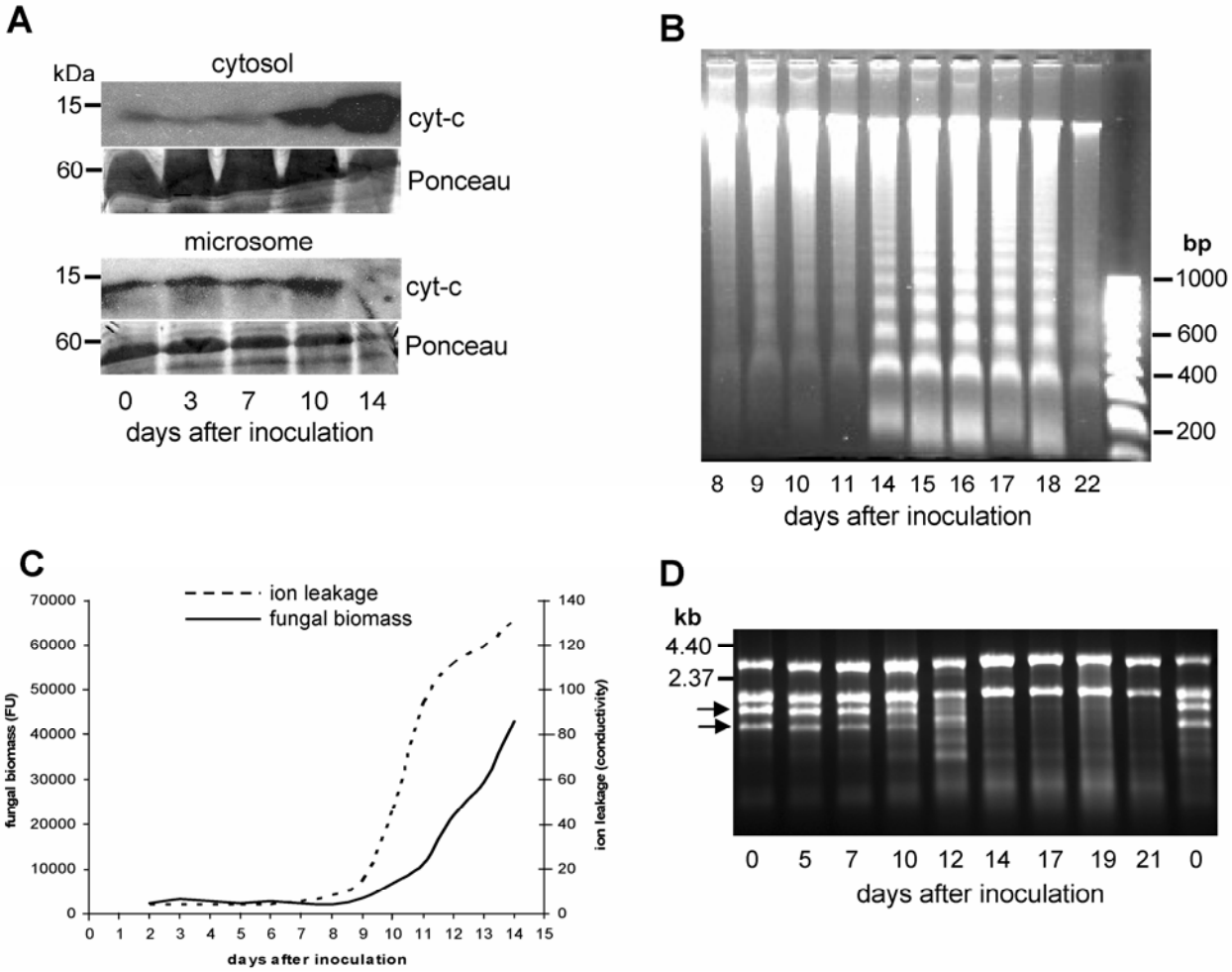

Fig. 3. Disease symptom development has features of programmed cell death and promotes an increase in fungal growth rate. **A,** Cytochrome c moves from the mitochondria to the cytosol as disease symptoms develop. Western blot of cytosolic proteins (upper panel, approximately 100 μg per lane) and microsomal fraction (lower panel, approximately 15 μg per lane) isolated at various stages of infection of inoculated leaves. Ponceau S–stained regions of approximately 60 kDa are shown as loading controls. **B,** Internucleosomal DNA cleavage is associated with symptom development. Total genomic DNA was isolated from inoculated leaves at various timepoints and resolved on agarose gels. The size difference between fragments is approximately 180 bp. **C,** Increases in ion leakage precede increases in fungal biomass. Infected leaves were taken at various timepoints following inoculation and were assayed for membrane integrity via-ion leakage assays (dashed line) or total genomic DNA was isolated and used as template for real-time polymerase chain reaction in order to measure fungal biomass (solid line). **D,** Analysis of total RNA isolated from infected leaves on various days after inoculation identifies a sudden disappearance of host chloroplastic rRNA species (arrows) across the transitional period.

4B. Principal component 1 was found to account for 99.3% of the variance in the data and emphasizes that day 13 fungal-inoculated, and to a lesser extent day 9 fungal-inoculated samples, represent the most distinct samples of the six assayed (three mock- and three fungal-inoculated). The loadings plot (not shown) indicates that principal component 1 describes an increase in all the peaks in the spectrum except those belonging to sucrose.

Fungal microarray analysis identifies a nutrient-limited slow-growth state prior to the advancement of host PCD.

The data described above have shown clear differences in host physiology to which *M. graminicola* successfully adapts during infection. We have used fungal transcription profiling to investigate these adaptations using a cDNA microarray, the quality of which was established in previous studies (Keon et

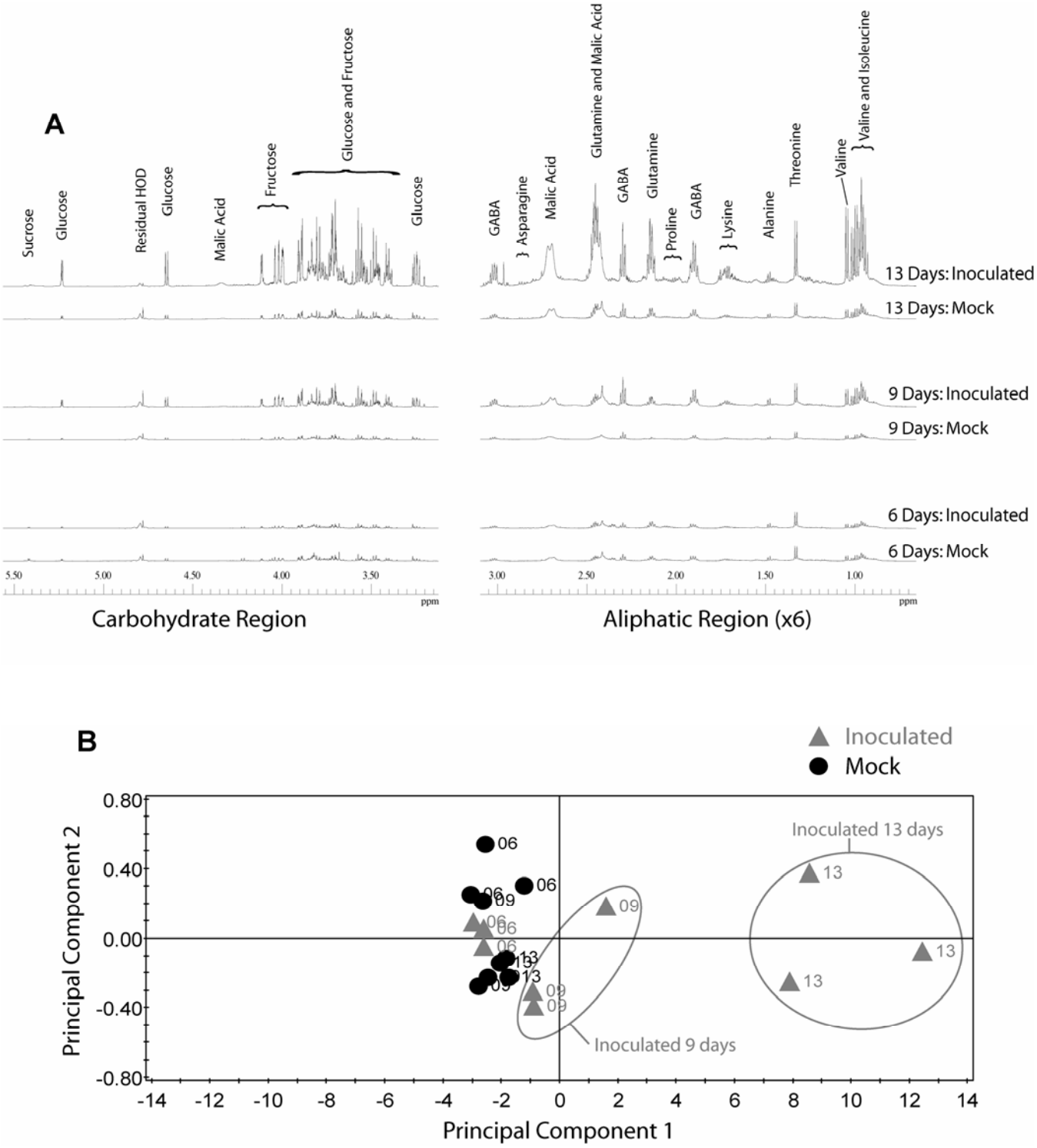

Fig. 4. [1]H-nuclear magnetic resonance (NMR) analysis of apoplastic metabolites during phases of infection. **A,** Aliphatic and carbohydrate regions of the NMR spectra of the inoculated and mock-inoculated samples. Each spectrum is the average of the three replicates. **B,** Scores plot from principle component analysis of NMR spectral data showing inoculated (circle) and mock-inoculated (triangle) samples (06 = 6 days, 09 = 9 days, and 13 = 13 days after treatment).

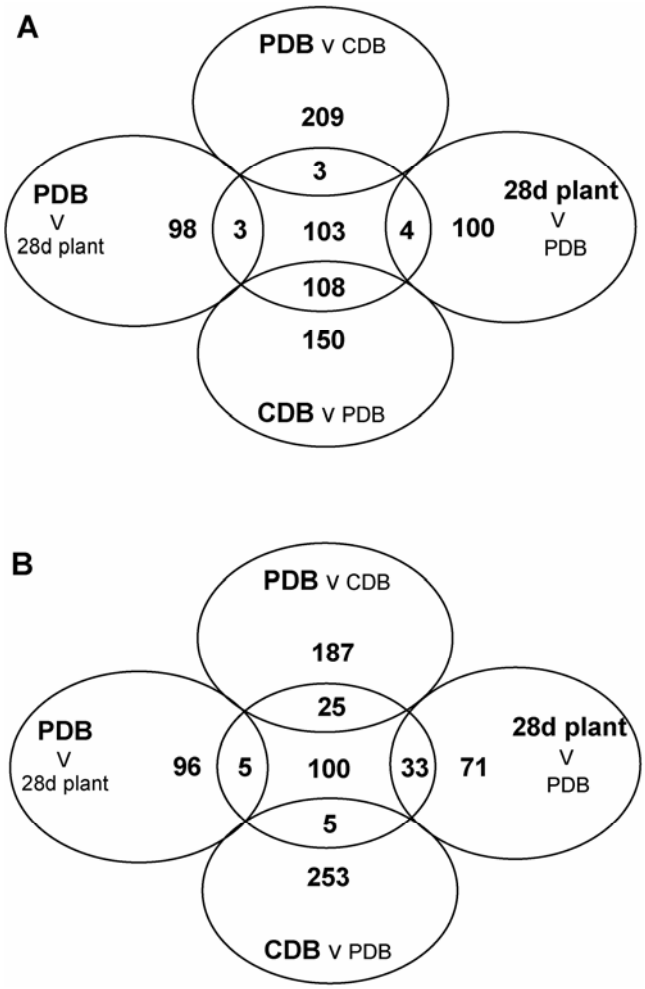

Fig. 5. Overlap of differentially expressed fungal gene set with previous experiments identifies a starvation state at day 9 or 10 of infection. **A,** Overlap of the 217 genes more highly expressed at day 9 or 10 with those differentially expressed in previous studies. **B,** Overlap of the 158 genes more highly expressed at day 14 with those differentially expressed in previous studies. Note that cumulative numbers of genes within the central circles is larger than the total number described as differentially expressed due to particular genes falling in more than one overlapping segment.

al. 2005b). Our preliminary work demonstrated a requirement to increase the stringency of the hybridization conditions in order to prevent cross-hybridization of closely homologous plant sequences to the fungal microarray. These modifications are described in the methods. During these studies, we first attempted to compare inoculated leaf material at day 6 with that at day 9 or 10. We were only able to detect very weak and selected hybridization to the array from the day 6 material, which prevented a meaningful microarray study. This confirmed our real-time PCR analysis on fungal biomass, which indicated that relatively little fungal growth had occurred by day 6. Sufficient growth had occurred, however, by day 9 or 10 to enable a transcriptional analysis. We directly compared 9- or 10-day versus 14-day infected leaf material, using two biological repeats hybridized at high stringency to 16 replicate microarray blocks, and set a threshold of a twofold change at a significance level of $P < 0.01$ for data interpretation.

Genespring analysis of the final datasets identified 217 fungal genes more highly expressed at day 9 or 10 than day 14 and 158 genes more highly expressed at 14 days. We first compared this dataset with those generated from previous experiments (Keon et al. 2005b) to see whether and to what extent the identity of the differentially expressed genes may overlap. Key amongst these previous datasets were those comparing *M. graminicola* log phase growth in vitro in a rich complex medium (potato dextrose broth [PDB]) with that in medium that supported only slow growth (Czapek-Dox broth [CDB]). *M. graminicola* was shown to grow approximately five times faster in PDB. We also compared growth in PDB with 28-day infected leaf material (late-stage infection). Startlingly, among the 217 genes identified as more highly expressed at day 9 or 10 in this study, over 50% (108 genes) were previously detected to be more highly expressed in fungus growing in CDB than in PDB (Fig. 5A). Statistical analysis indicated this overlap to be highly significant ($P < 0.001$). CDB has sucrose as a C source and nitrate as a sole N source. In order to further interpret our current data more precisely, we sought to identify exactly what was the limiting factor by supplementing additional C and N sources to CDB and measuring fungal growth in vitro. Nitrate represents a poor N source for *M. graminicola*, as growth is substantially improved by the addition of more favorable N sources, including ammonium and amino acids (gamma aminobutyric acid). It is, therefore, possible that a number of the

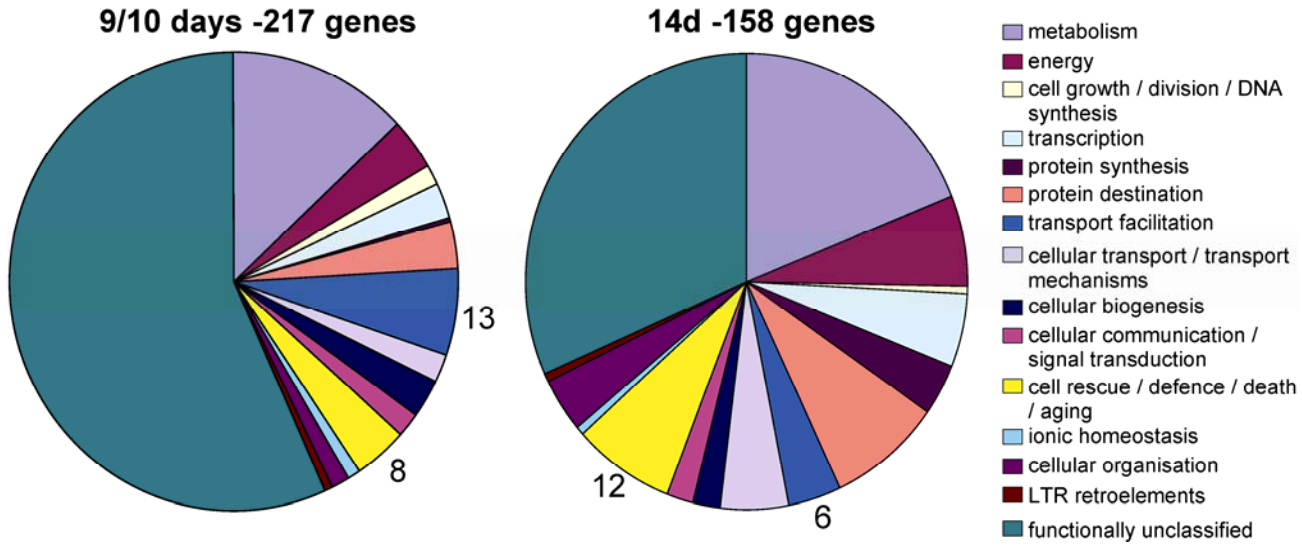

Fig. 6. Functional categories of the differentially expressed genes. Genes were classified according the MIPS scheme. The segments highlighted with numbers are described in greater detail in Tables 1 and 2.

genes previously identified as more highly expressed during growth in CDB than in PDB arise as a consequence (both direct and indirect) of the presence of only a relatively poor N source. The majority of the remaining genes more highly expressed at day 9 or 10 postinoculation were unique to this condition (103) and, thus, had not been detected as differentially expressed in previous studies.

Importantly, the reciprocal situation was seen when an analysis of overlap of the 158 genes more highly expressed at 14 days was performed (Fig. 5B). In this case, there was almost no overlap with genes more highly expressed in CDB versus PDB. Instead, 25 genes were also identified as being more highly expressed in PDB than CDB and 33 were previously identified as being more highly expressed in 28-day infected leaf material (late stage) compared with growth in PDB. Statistical analysis again determined this overlap to be highly significant ($P < 0.001$ in both cases). As late-stage infected plant material was also shown in previous studies to provide a nutrient-rich environment for fungal growth (Keon et al. 2005b), the overall dataset indicates an alleviation of a nutrient-limiting slow-growth state in the fungus as host cell death accelerates across the transitional period.

The differentially expressed fungal genes involved in transport and cellular stress.

We next analyzed the differentially expressed genes according to MIPS functional categories (Fig. 6). Of the 217 genes more highly expressed at day 9 or 10 over 50% were functionally unclassified (having no significant homology to any gene of known function or having homology to genes of unknown function). This category represented only a third of the genes more highly expressed at 14 days. Notably, the functional categories shown in Figure 6 include protein synthesis and protein destination, which were more prevalent among the genes more highly expressed at 14 days and may be explained by the accelerated growth at this stage. Genes involved in transport facilitation were among those more highly expressed at 9 or 10 days. Table 1 shows that this class comprised genes potentially involved in nutrient uptake and detoxification processes including carbohydrate, amino acid, ATP-binding cassette, and major facilitator transporters. These activities were not represented in the genes more highly expressed at day 14.

Genes from the functional category cell rescue and defense were more prevalent among those more highly expressed at 14 days. Table 2 shows a clear difference between the predicted

Table 1. Differentially expressed fungal genes involved in transport mechanisms

Gene[a]	MIPS code	Classification	Function
Day 9 or 10*			
mg[0740]	7	Transport facilitation	Stomatin-like protein (membrane protein)
mgc20d09f	7	Transport facilitation	Transporter
mg[1321]	7.07	Sugar, carbohydrate and metabolite transporters	Maltose permease
mg[0530]	7.07	Sugar, carbohydrate and metabolite transporters	Sugar transporter
mg[0934]	7.07	Sugar, carbohydrate and metabolite transporters	Hexose transporter
mg[0826]	7.1	Amino acid transporters	N amino acid transport system protein
mg[0655]	7.11	Peptide transporters	Peptide transporter
mg[0049]	7.22	Transport ATPases	Vacuolar proton pump
mgc11a04f	7.22	Transport ATPases	Plasma membrane H+-ATPase
mgb0610f	7.22	Transport ATPases	H+-transporting ATPase
mg[0212]	7.25	ABC transporters	ATP-binding cassette, ABC transporter
mgb0618f	7.28	Drug transporters	Multidrug-resistance 12-spanner family
mgc17c03f	7.28	Drug transporters	Major facilitator membrane transporter
Day 14*			
mg[0973]	7.07	Sugar, carbohydrate and metabolite transporters	Hexose transporter
mg[0038]	7.22	Transport ATPases	Plasma membrane H+ ATPase
mgc17g02f	7.22	Transport ATPases	Sodium P-type ATPase
mgc15h12f	7.99	Other transport facilitators	Mitochondrial carnitine carrier
mg[1067]	07.04.04	Other cation transporters (Na, K, Ca, NH4, etc.)	Potassium channel subunit
mg[0852]	07.04.04	Other cation transporters (Na, K, Ca, NH4, etc.)	Calcium-related spray protein

[a] * indicates that genes were more highly expressed at this timepoint.

Table 2. Differentially expressed fungal genes involved in cell stress

Gene[a]	MIPS code	Classification	Function
Day 9/10*			
mga1100f	11.07.01	Detoxification involving P450	Cytochrome P450
mgc11b12f	11.07.03	Detoxification by modification	Glutathione-*S*-transferase
mg[0341]	11.07.03	Detoxification by modification	Glyoxalase I
mg[0335]	11.07.03	Detoxification by modification	Bleomycin hydrolase
mg[0874]	11.07.03	Detoxification by modification	Lactoylglutathione lyase
mgc18f11f	11.07.03	Detoxification by modification	Glutathione *S*-transferase
Day 14*			
mgc05e09f	11.07.01	Detoxification involving P450	Cytochrome P450
mg[0986]	11.07.02	Defense against oxidative stress	Catalase A
mg[0784]	11.07.02	Defense against oxidative stress	Manganese superoxide dismutase
mg[0839]	11.07.02	Defense against oxidative stress	Peptide methionine sulphoxide reductase
mg[0170]	11.07.02	Defense against oxidative stress	Cu/Zn superoxide dismutase
mg[1350]	11.07.02	Defense against oxidative stress	Thioredoxin peroxidase (peroxiredoxin)
mg[1358]	11.07.02	Defense against oxidative stress	Thiol-specific antioxidant protein
mgc13a09f	11.07.03	Detoxification by modification	Rhodanese (thiosulfate sulfurtransferase)
mg[0597]	11.07.03	Detoxification by modification	Glutathione *S*-transferase

[a] * indicates that genes are more highly expressed at this timepoint.

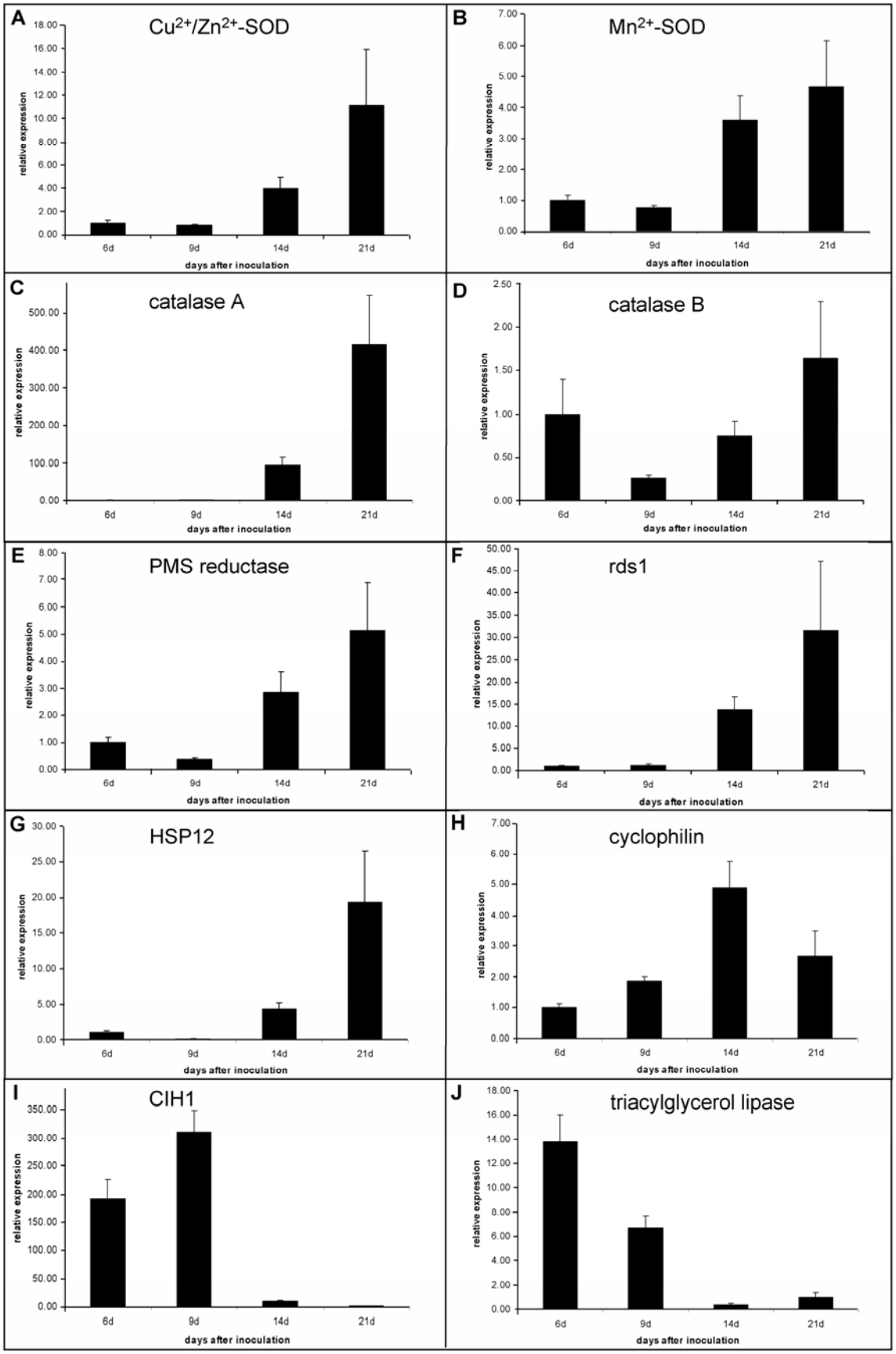

Fig. 7. Real-Time reverse transcriptase-polymerase chain reaction validation of differentially expressed fungal genes throughout the infection timecourse. **A** through **H,** The relative expression of various fungal genes involved in stress responses during host infection from day 6 to day 21. These genes were all shown to be more highly expressed at day 14 than at day 9 or 10 of infection in the microarray dataset. **I** and **J,** Confirmation of the expression of selected genes predicted to be more highly expressed at day 9 or 10 than at day 14 of infection in the microarray dataset. All data were normalized to the expression of beta-tubulin.

function of individual genes involved in stress adaptation that were differentially expressed at day 9 or 10 and day14. In the latter stage, the fungus has increased expression of a number of genes involved in oxidative stress biology, including catalases, superoxide dismutases, peptide methionine sulfoxide (PMS) reductases, and thiol peroxidases. A range of heat-shock proteins, including various molecular chaperones and peptidylprolyl isomerases (cyclophilins), were also more highly expressed at 14 days. In contrast, at day 9 or 10, the fungus appears to be engaged in chemical detoxification, particularly involving glutathione biology and high expression of glyoxalase 1 homologs, suggesting detoxification of methylglyoxal, a potentially toxic by-product of glycolysis (Table 2).

Fungal metabolic changes inferred from the gene expression data.

The major change in fungal metabolism described above appeared to support an apparent transition from a slow-growing state to rapid growth between days 9 or 10 and 14 of infection. The microarray dataset provides further supporting evidence for this transition in the form of differentially expressed genes known to be regulated by nutrient status. For example, genes known to be repressed in high nutrient environments, including phosphoenolpyruvate carboxykinase and acetyl-CoA synthetase, were more highly expressed at the day 9 or 10 timepoint. Conversely at 14 days, the fungus appeared to have responded to the increased availability of nutrients with higher expression of genes involved in energy production, highlighted by increased expression of genes encoding a number of ATP synthase subunits. Genes encoding various proteases including aspartic, serine, and aminopeptidases were also more highly expressed at 14 days.

Two independent sequence homologs of glyoxalase 1 were more highly expressed at day 9 or 10. These enzymes act to detoxify methylglyoxal produced as a by-product of the triosephosphate isomerase catalyzed interconversion between glyceraldehyde-3P and dihydroxyacetone phosphate within glycolysis. Perhaps significantly, a gene encoding triosephosphate isomerase was also more highly expressed at day 9 or 10. One input to the production of dihydroxyacetone phosphate that can often be used to fuel glycolysis or gluconeogenesis is the degradation of glycerol that can be produced as a consequence of the metabolism of lipids (triacylglycerols). A triacylglycerol lipase was also more highly expressed at day 9 or 10, suggesting that the fungus may be utilizing stored lipids during the symptomless slow-growth phase of infection. This pathway might then lead to a consequent increase in methylglyoxal to be detoxified by the glyoxalase system. Other notable features were the coordinate higher expression at day 9 or 10 of an acetate regulatory DNA-binding protein homologous to *A. nidulans FacB* with genes encoding acetamidase and acetyl-CoA synthetase. This coordinate regulation is a characteristic of the metabolic utilization of acetate by fungi, whereby *FacB* and its homologs positively control the expression of the latter two enzymes. Levels of cytosolic acetyl-CoA for fatty acid and sterol biosynthesis may also be maintained through expression of ATP citrate lyase at days 9 or 10 of infection.

Fungal gene expression at both earlier and later timepoints of plant infection.

In order to validate the expression changes from the current microarray experiment and to investigate the expression levels of particular genes at both earlier (day 6) and later (day 21) stages of infection, we used a real-time reverse transcriptase (RT)-PCR approach. Figure 7 shows the results of this analysis for 10 independent fungal genes that microarray analysis predicted to change in expression between days 9 or 10 and 14 of infection. Eight of the 10 genes selected for analysis are predicted to function in oxidative (singly or in combination with other) stress responses. Six of these, Cu^{2+}/Zn^{2+}-SOD, Mn^{2+}-SOD, catalase A, PMS reductase, rds1, and HSP12, had very similar expression profiles (Fig. 7 A, B, C, E, F, and G) in that they all displayed an initial increase in expression at day 14 of infection and a further increase by day 21 (very late-stage infected plant material with heavy sporulation). The overall level of expression of the catalase A gene in the 21-day material reached approximately 400-fold of that seen during the earlier symptomless-growth phase (days 6 and 9; Fig. 7C). Interestingly, a second catalase transcript, described as catalase B, did not respond in the same way. Although nominally most highly expressed at day 21, the actual fold changes relative to the other timepoints was much less dramatic and insignificant with respect to the expression level determined at day 6 of infection (Fig. 7D). The expression level of a cyclophilin gene was shown to peak at 14 days during this analysis (Fig. 7H).

Other genes were confirmed to be more highly expressed during the earlier phases of infection (days 6 and 9). Figure 7I shows the expression profile for a transcript with most sequence homology (albeit weak, blastx of 2e-05) to the biotrophy-associated gene *CIH1* from *Colletotrichum* species (Perfect et al. 1998), which the microarray dataset predicted to be the fungal gene with the highest expression at day 9 or 10 relative to that at day 14. The PCR analysis confirmed this pattern of expression and also demonstrated high expression of this gene at the earlier timepoint (day 6). Similarly, as described earlier, a triacylglycerol lipase was predicted to be more highly expressed at day 9 or 10 than at day 14. This was confirmed to be the case in the PCR analysis, which also demonstrated the gene to be even more highly expressed at the earlier phase of infection (Fig. 7J). This may reflect the continued use of stored lipids as nutrient sources during symptomless growth, which is subsequently rendered obsolete as host PCD develops further and facilitates necrotrophic fungal nutrition. Overall a good correlation was seen between the gene-expression levels determined by both microarray and RT-PCR analyses.

DISCUSSION

Our experimental system has allowed us to investigate a key feature of host-pathogen interactions between plants and microbes—namely, how and to what extent the invading pathogen is able to respond to changes in host physiology during particular stages of infection. In this paper, we have used attached-leaf infection assays in order to simultaneously study both host and pathogen physiology during a disease transition.

The development of disease symptoms in the host has features of HR-like PCD.

Symptoms of *M. graminicola* infection of wheat appear first as chlorosis and necrosis immediately preceding the development of pycnidia and asexual sporulation. The earliest visible disease symptoms appear as small water-soaked regions, typically 8 days after inoculation. These are replaced by pitted necrotic specks the following day, the overall transition taking no more than 16 h. This very rapid and strictly localized form of cell death is a characteristic of the HR of plants to pathogens during race-cultivar specific resistance (Hammond-Kosack and Jones 1996) and also in response to general elicitors produced by various pathogens (Boller 1995). The process is supported by illumination, which plays a positive role in leaf chlorosis and the formation of necrotic lesions. Light has long been described to be an accelerating or necessary feature for developing disease symptoms on plants infected by a range of leaf spot or blotch-type fungal pathogens (Calpouzos and

Stallknecht 1967; Rotem et al. 1988). Its role in various forms of plant cell death has been suggested to arise from effects on the redox balance of cells that are already subjected to another form of environmental stress (Bechtold et al. 2005; Karpinski et al. 2003). Illumination has recently been demonstrated to play an important role in HR-associated cell death triggered downstream of increases in H_2O_2 in tobacco leaves following elicitation (Montillet et al. 2005) and during effective resistance to plant viruses (Chandra-Shekara et al. 2006). We have also demonstrated here that the water-soaked lesion phenomenon is associated with increased levels of superoxide in the affected regions. Although further work is required to elucidate the origins of these ROS, these features are often seen during HR-like plant cell death, placing perturbations in the redox status of mesophyll cells at the forefront of symptom development during this phase of fungal infection. Using illumination as an orientation feature for the development of symptoms also has the added effect of ensuring that the majority of pycnidia that subsequently develop form in an area of the leaf best suited to be exposed to rainfall and thus maximizes the ability of the fungus to spread asexually throughout the canopy via splash-mediated distribution of pycnidiospores.

Our study has shown that the development of necrotic symptoms is tightly linked with a dramatic loss of membrane integrity detectable through ion-leakage studies. An unexpected feature of symptom development was the clear appearance of a host DNA-fragmentation response as characteristic laddering of approximately 180-bp internucleosomal fragments detectable on agarose gels. This phenomenon is typical of PCD reactions originally associated with apoptosis in animal cells (Nagata et al. 2003) and subsequently also shown for various types of plant cell death (Ryerson and Heath 1996). In animals, this response is mediated by the activation of a specific nuclease downstream of the activation of cysteine protease (caspase) cascades, the whole process being orchestrated by the mitochondria (Ravagnan et al. 2002). Plants lack sequence homologs of many of these cell-death effectors but do appear to possess functional equivalents. For example, a DNase has been identified in the intermembrane space of plant mitochondria that may function in triggering downstream PCD events (Balk et al. 2003). Similarly, cysteine protease activities have been implicated in various forms of plant cell death and particularly during plant-pathogen interactions (Chichkova et al. 2004; Coffeen and Wolpert 2004; del Pozo and Lam 1998; Hatsugai et al. 2004; Woltering 2004). Thus far, we were unsuccessful in detecting elevated caspase-like activities preceding the DNA fragmentation response in our system, using assays based on the cleavage of fluorescently labeled substrates. However, the success in detecting these activities is very dependent on assay conditions and the type of caspase substrate used, and we cannot, therefore, rule out their involvement in symptom development.

Plant PCD is also often associated with the release of mitochondrial cytochrome c into the cytosol of dying cells (Balk and Leaver 2001; Balk et al. 1999; Jones 2000; Krause and Durner 2004; Tiwari et al. 2002; Yao et al. 2004; Zuppini et al. 2005). During apoptosis in animals, this triggers the activation of the protease pathways resulting in DNA fragmentation. We also identified cytochrome c release occurring as one of the earliest biochemical events in the PCD response. Our results therefore support those of others who have suggested that PCD pathways of plants and animals share mechanistic similarities, despite quite often lacking clear sequence homologs of the active molecular participants. It remains to be conclusively shown that the observed cytochrome c release triggers downstream cell-death responses in plants. However, several articles have shown that antiapoptotic proteins that target the mitochondria or caspase activity when expressed in plants provided resistance to necrotrophic fungi and fungal toxins (Lincoln et al. 2002). Similarly, effective HR-mediated resistance of barley to the biotrophic fungus *Blumeria graminis* was attenuated by overexpression of a native antiapoptotic Bax inhibitor-type protein (BI-1) (Huckelhoven et al. 2003), suggesting that similar mechanisms, centered around the mitochondria, operate in triggering cell-death processes in both plants and animals. Our data suggests that overexpression of antiapoptotic-type proteins might also serve to prevent the switch to necrotrophic growth of *M. graminicola*, a hypothesis that will be investigated in the future. Overall, it is clear that the development of symptoms is, in fact, a form of host PCD involving rapid loss of cell integrity and the degradation of host macromolecules (DNA, RNA, protein, and other cellular components). It appears that this type of aggressive cell death is ineffective in containing the spread of *M. graminicola* and, rather, may facilitate its increased growth rate and transition towards sporulation by providing a rich source of nutrients utilizable via a switch to necrotrophic nutrition.

There is a lack of evidence for biotrophic feeding during the symptomless-growth phase.

The apoplastic metabolite analysis performed in this study indicated that, during the symptomless phase of the interaction, the basic nutrient composition is neither increased (as was reported for the biotrophic tomato-leaf pathogen *Cladosporium fulvum* [Solomon and Oliver 2001]) nor depleted to any measurable level due to the presence of the fungus. As we were also unable to detect any measurable increase in fungal biomass during this phase, this argues against *M. graminicola* behaving as an effective biotroph. This also suggests that the trigger for host PCD is unlikely to be a massive depletion of nutrients in the apoplast surrounding the mesophyll cells. The only changes in apoplastic metabolite content detected in this study were seen following the onset of host PCD when it became enriched for a whole range of amino acids and sugars, presumably due to leakage from the host cells as membrane integrity was lost. This represents a substantial (and perhaps previously unavailable) potential nutrient source to the fungus, which may support the increase in growth detected following the onset of host PCD.

Although the *M. graminicola* microarray is lacking a substantial number of genes expected to make up the full genome of this organism, we and others have shown in previous studies that certain metabolic changes in plant pathogenic fungi can be inferred through differential expression of key regulatory genes (Both et al. 2005; Keon et al. 2005b). The dramatic overlap of genes expressed at day 9 or 10 with those previously identified as being more highly expressed during slow growth in a nitrogen-limiting broth clearly demonstrates that, at this stage, the fungus is residing in an environment that is nutritionally poor relative to the environment encountered during advanced host PCD. The expression levels of various genes known to be affected by nutrient supply support this conclusion. For example, many metabolic genes known to be repressed by high nutrient levels were seen to be more highly expressed at day 9 or 10 in this experiment, including phosphoenolpyruvate carboxykinase and acetyl-CoA synthetase. The latter is coordinately regulated along with acetamidase via the DNA-binding protein *FacB* in *Aspergillus nidulans* (Todd et al. 1997). Homologs of these genes were also more highly expressed at day 9 or 10, suggesting the fungus to be effectively metabolizing acetate at this stage. The biosynthetic means to synthesize essential fatty acids from acetyl-CoA in the cytosol is also possibly aided by higher expression of ATP citrate lyase at this timepoint.

A gene encoding triacylglycerol lipase was most highly expressed during the symptomless phase of infection (day 6 and,

to a lesser extent, day 9). This may suggest the use of internal lipid stores in providing energy right up to the point of host PCD. Plant-pathogenic fungi are believed to utilize stored compounds including lipids as energy sources for growth in nutrient-depleted environments and often to enable the formation and function of host penetration structures (Beilby and Kidby 1980; Both et al. 2005; Solomon et al. 2004). As *M. graminicola* does not appear to use physical penetration structures then, one might assume that, if large stores of lipids were available, they could support the growth of the fungus for a significant period of time during host colonization, thus negating the requirement for the biotrophic assimilation of host nutrients. Contrary to this, however, are reports that *M. graminicola* spores germinated on glass slides generated very little hyphal material in the absence of an external nutrient source (Duncan and Howard 2000). Nevertheless, our fungal growth, gene expression, and apoplastic metabolite analysis provides little support for biotrophic feeding during the symptomless phase. However, what remains clear is that the advancement of host PCD greatly increases the supply of nutrients to the fungus and may provide it with the necessary energy to support more rapid growth and asexual sporulation.

Possible involvement of the fungus in inducing host cell death.

As shown in this study the symptomless-growth phase of *M. graminicola* is unusually long (8 days following heavy inoculation). During this period, fungal biomass remains low, with measurable increases only occurring following the development and advancement of disease symptoms. The overlap in the identity of fungal genes more highly expressed at day 9 or 10 with those previously shown to be more highly expressed in CDB (described as a nutrient-limiting medium) than in PDB (complex nutrient-rich medium) indicates that the fungus is in a nutritionally limited state immediately before and during the early stages of symptom development. CDB supports only limited growth of *M. graminicola*, due to having nitrate as the sole N source, and therefore, many of the differentially expressed genes in this comparison may possibly have originated due to a slow growth phenotype in a nitrogen-limiting environment. We have shown that the slow-growth phase ends following the onset and advancement of host PCD. The synchronicity of this response suggests the fungus might play a role in triggering host PCD. As we have no evidence to suggest that PCD is triggered by a significant depletion of apoplastic metabolites during the symptomless-growth phase, an alternative trigger might be the release of some form of fungal toxin or elicitor.

Host cell death–inducing factors have been described to be produced by fungal pathogens under starvation conditions, frequently in response to nitrogen starvation (Van den Ackerveken et al. 1994). Disease symptom development in rice leaves infected with *Magnaporthe grisea* was also suggested to result as a consequence of fungal N-starvation (Talbot et al. 1997). It has previously been suggested, but never proven, that *M. graminicola* may produce some kind of host-specific toxin or elicitor to initiate host cell death and facilitate sporulation (Kema et al. 1996). Many fungal pathogens causing diseases on various plant species are known to produce host-specific toxins that are often activated, or positively influenced to induce host cell death, by light (Daub and Ehrenshaft 2000; Navarre and Wolpert 1999a; Stone et al. 2000). Proteinaceous toxins known to induce cell death in wheat have also been isolated from the necrotrophic fungus *Pyrenophora tritici-repentis* and have been shown to target the chloroplast of sensitive cultivars (Manning and Ciuffetti 2005). The possibility of a starvation state existing at the end of the symptomless-growth phase (day 9 or 10) would support a model by which the fungus was suddenly required to produce a HR-inducing toxin or elicitor in order to increase its nutrient supply and facilitate asexual sporulation. The fact that noninoculated regions of infected leaves (including the leaf tips) remain green throughout the development of advanced symptoms, suggests that, if such an agent is produced, then it is not freely diffusible. An alternative explanation to the production of a toxin may be that the fungus simply surpasses a critical level of growth whereby the host recognizes a number of general surface or secreted elicitors that trigger events resulting in the HR-like cell death often seen in some forms of plant innate immunity (Nurnberger and Lipka 2005). However, we were unable to measure what may be subtle increases in fungal biomass (Kema et al. 1996) towards the end of the symptomless-growth period, using our real-time PCR assay.

Surviving and benefiting from the HR.

The accelerating PCD of the host appears to enable the fungus to remove itself from a slow-growing state and begin the process of generating its asexual sporulation machinery on the illuminated (light-facing) surface of the infected leaf. As the 14-day timepoint taken for microarray analysis contains leaves with immature pycnidia, it is possible that some of the genes up-regulated at this timepoint may be specifically associated with pycnidial development. A large number of the differentially expressed genes at both days 9 or 10 and 14 also suggest specific adaptive processes initiated in order to tolerate the potential stresses imposed upon the fungus at each stage. HR-like cell death has long been associated with increased levels of ROS in and around the affected regions. The roles of ROS in plant-pathogen interactions are complex and often appear dependent upon the type of interaction. For example, biotrophic fungi are thought to be effectively managed by plants via the generation of ROS and localized cell death (Glazebrook 2005), whereas necrotrophic pathogens appear well suited to cope with this type of response and have often been described to benefit from it (Glazebrook 2005; Govrin and Levine 2000). Overall, levels of ROS (H_2O_2 and O_2^-) increased from day 9 or 10 to day 14 in our bioassay. However, the origin of these increases remains to be determined. Our microarray data showed a simultaneous adaptation in the fungus by way of increased expression of genes encoding a diverse range of activities that counteract oxidative stress including, catalase A, Cu^{2+}/Zn^{2+}-SOD, mitochondrial Mn^{2+}-SOD, PMS reductase, peroxiredoxin, and a thiol-specific antioxidant protein. Future studies will generate deletion mutants for these genes to ascertain their relative importance for surviving the developing host cell death.

Previous studies have shown that high levels of ROS are seen during susceptible interactions at the onset of visible symptoms (Shetty et al. 2003) and are associated with mature pycnidia even when the leaf is completely senesced at very late stages of disease (Keon et al. 2005b). Many stress response genes were highly expressed at day 14 and even more so at day 21 when compared with the symptomless stage of infection. The expression of catalase A provided a dramatic example. In at least one other fungus originally described as hemibiotrophic, *Colletotrichum gloeosporioides*, a similar high-level expression of a catalase gene has been reported during the necrotrophic phase of nutrition (Goodwin et al. 2001). In some other fungi, catalase A homologs have been shown to be expressed at very high levels in spores (Bussink and Oliver 2001; Hisada et al. 2005), and therefore, it is possible that the expression pattern described here reflects the maturation of pycnidia and heavy sporulation in the day 21 material. If this holds true, then genes of this type may prove to be very useful for monitoring the onset of sporulation in infected tissues.

The immature pycnidia present in the day 14 material used in this study also stain strongly for ROS. At present, we cannot distinguish whether the ROS detected at this stage is of plant or fungal origin. It remains possible that the oxidative stress genes more highly expressed at day 14 form part of a developmental program involving ROS and, thus, may not be triggered as a consequence of perceiving increased ROS in the immediate environment. It is also possible that fungus-generated ROS may play a role in one or both the development or maturation of pycnidia, as has been reported for the development of sporulation structures in other fungi (Lara-Ortiz et al. 2003; Malagnac et al. 2004).

Concluding remarks.

Many fungal pathogens of important crop plants have lifestyles similar to that described for *M. graminicola*, in that they have a relatively long period of symptomless association prior to necrotrophic growth in dying or dead plant tissue. Recent phylogenetic analyses place *M. graminicola* among other important plant pathogens causing leaf spot or blotch diseases on plants of great agricultural significance, including bananas (*Mycosphaerella fijiensis*) and maize (*Cercospora zeae-maydis*) (Goodwin 2004). These fungi exhibit similarities in infection including stomatal penetration, long periods of symptomless colonization, a lack of obvious specialized feeding structures, and ultimately, the formation of chlorotic or necrotic lesions in which they sporulate. Here, we have described a study of the transition to disease symptom development from the point of view of both the host and the pathogen. It has become apparent that the switch in fungal-growth state may be facilitated by a strictly localized form of host PCD, similar in its characteristics to the HR. Therefore, symptom development is more than simply host "cell collapse" and, rather, occurs in a coordinated manner as the host appears to trigger a delayed defense response that is inappropriate for the containment of this particular pathogen. It will now be interesting to determine whether host PCD mechanisms underpin these transitions for related fungi and, thus, represent possible targets for broad-ranging disease control.

MATERIALS AND METHODS

Plant and fungal material and handling.

M. graminicola isolate IPO323 (Netherlands) was used in all experiments. The isolate was stored at –80°C in 50% (vol/vol) glycerol. Fungal spores for plant inoculation were harvested from 7-day-old cultures growing (budding) on YPD plates (Oxoid Ltd., Hampshire, U.K.) at 15°.

For plant infection, the second leaf of 17-day-old wheat seedlings (cultivar Riband) was attached, adaxial side up, to Perspex sheets using double-sided tape. The leaves were inoculated evenly with fungal spores at a density of 10^7 cells per milliliter in water containing 0.1% (vol/vol) Tween 20. Following an initial 72-h incubation at 100% relative humidity, inoculated plants were incubated at 16°C with a 16-h light period at 88% relative humidity for up to 21 days. After 21 days, many pycnidia were visible on inoculated areas of the leaf and the surrounding leaf tissue was senescent. Infected tissues were excised at various timepoints after inoculation and were stored at –80°C for RNA isolation and microarray analysis or were immediately used to generate protein fractions or were used in ion-leakage and staining procedures.

For in vitro N source growth experiments, *M. graminicola* was grown either in a basal medium of bacto yeast nitrogen base without amino acids or ammonium sulphate (Difco), buffered to pH 6.0 with 50 mM MES, or CDB buffered in the same way. Sources of carbon and nitrogen were each added to the final concentrations. Culture medium (100 ml) were inoculated with 2×10^4 sporidia per milliliter and were incubated with shaking (220 rpm) at 21°C for 5 days. Growth was measured as the dry weight of mycelium. For an estimation of dry weight the cultures were harvested onto preweighed filter disks and were dried at 60°C. Cultures with the addition of glucose, potassium nitrate, or ammonium sulphate alone failed to grow.

Western blotting.

Crude cytosolic and microsomal fractions were generated as described by Krause and Durner (2004). Eight inoculated leaves (5 cm each) were homogenized and filtered through two layers of Miracloth. The extract was then centrifuged at 4°C for 15 min at 13,200 rpm to pellet the crude microsomal fraction. The supernatant was taken as the cytosolic fraction. The microsomal pallet was washed in 1 ml of extraction buffer and recentrifuged. The pellet was then disrupted by grinding in 100 µl of extraction buffer containing 0.1% (vol/vol) Tween 20. After recentrifugation, the supernatant was taken as the crude microsomal fraction. Protein extracts (approximately 100 µg cytosolic and approximately 15 µg microsomal) were then separated on 15% sodium dodecyl sulfate (SDS) polyacrylamide gel electrophoresis plates and were blotted onto Hybond ECL nitrocellulose (Amersham Pharmacia, Uppsala, Sweden). Blots were probed with a 1:2,000 dilution of monoclonal anti-cytochrome c antiserum (clone 7H8.2C12; BD Biosciences, San Jose, CA, U.S.A.) and subsequently 1:5,000 dilution of anti-mouse IgG horse-radish peroxidase (Sigma, St. Louis). Blots were developed using chemiluminescence (ECL-plus; Amersham).

Ion-leakage assays.

All assays were performed in triplicate. Two leaves (approximately 5 cm) from inoculated or control-treated plants were added to 10 ml of deionized water (bathing solution). Leaves were then vacuum-infiltrated (four times for 30 s) at 25 mbar pressure with complete release of vacuum in between. The infiltrated leaves were then allowed to stand in the bathing solution for 1 h at room temperature, after which the leaves were removed, the bathing solution was vortexed, and the ionic strength was monitored using a conductivity meter.

^{1}H-NMR analysis of apoplastic metabolites.

Six wheat leaf segments (5 cm long) from inoculated or mock-inoculated control plants were placed in 75 × 10 mm acrylic test tubes. A 3.5-ml aliquot of deuterium oxide (D_2O) was added to each tube, which was then subjected to a vacuum of 50 mbar in a centrifugal evaporator for 10 min, to fully infiltrate each leaf. The tubes were then capped and rocked gently at 15°C for 30 min. The supernatant was poured off, and the leaves were gently blotted with absorbent paper to remove surface fluid before being placed in a test tube (as above) with the tip pierced. Each tube was placed in a 15-ml conical bottomed tube and was centrifuged at 1,000 × *g* for 5 min in a swing-out rotor. The volume collected ranged from 85 to 150 µl. This was transferred to an Eppendorf tube and was centrifuged at 16,000 × *g* for 3 min at room temperature. From each spun tube, 80 µl was transferred to a fresh tube, avoiding insoluble material, and 800 µl of D_2O was added. Each sample (750 µl) was transferred to a 5-mm NMR tube. To each tube was added 25 µl of D_2O containing 0.05% wt/vol TSP-d_4 (sodium salt of trimethylsilypropionic acid). ^{1}H NMR spectra were recorded at 300.000 on a Bruker Avance (Coventry, U.K.) spectrometer at a frequency of 600.053 MHz, using an inverse 5-mm probe. Each spectrum consisted of 1,024 scans of 64,000 datapoints and a spectral width of 7,310 Hz. The residual water signal was suppressed by presaturation during the 5-s relaxation de-

Table 3. Primers used in the real-time reverse transcriptase-polymerase chain reaction

Gene	Forward primer	Reverse primer
Cu^{2+}/Zn^{2+}-SOD	For 5′-ACATATACCAAACACCGCCACAATG	Rev 5′-TTAAGCAGCGATGCCAATGACA
Catalase B	For 5′-CCGAGATTGAGCAAATTGCGTT	Rev 5′-TCCCATTTCTTCTCGGCGAAG
PMS reductase	For 5′-ATCTTGATTTTGTCTGCATGCGG	Rev 5′-ACCGCAGTGGGATTTTCTACCA
HSP12	For 5′-CCGACTCTCTCAAATCTGCAGGA	Rev 5′-GGCCATGACTACCAAAATGTCGA
Cyclophilin	For 5′-AGTTCATGCTCCAGGGTGGTGA	Rev 5′-TACGAAGCACCAGCACCGGT
rds1	For 5′-TACCAGGAATGGATCGAGCTTGA	Rev 5′-GATGAAGCCCCAAACACCAGACT
Mn^{2+}-SOD	For 5′-AGAACCTCGCACCCAAGGCT	Rev 5′-ATGCTCCCACGCGTCGATAC
Catalase A	For 5′-GGTTGTCTACGAGCGCATGTCTC	Rev 5′-GAGCCTTCAATGCAGCCACAA
CIH1	For 5′-GCCACCAACTCCCAGACATACGT	Rev 5′-CGACAACCCTCAGAACACACTCC
Triacylglycerol-lipase	For 5′-AAACCGCTGGTCGTCGTCAA	Rev 5′-AAGTGGCAGTGCACCCAACG
Beta-tubulin	For 5′-ATCACCAGCCCGCAAAGCTT	Rev 5′-ACGATCTTGTGTCCGAGTACCAGC

lay. The FIDs were Fourier transformed after the application of an exponential window function with a line broadening of 0.5 Hz. Spectra were referenced to TSP-d_4 at 0.00 ppm. Phasing and baseline correction (2nd order polynomial) were carried out under automation. Metabolites were assigned by comparison with a library of known standards run on the same machine.

For PCA analysis, the ^{1}H-NMR spectra were reduced to ASCII files using AMIX (v3.6, Bruker Biospin). Spectral intensities were scaled to the TSP-d_4 peak and were reduced to integrated regions or "buckets" of equal width (0.01 ppm), corresponding to the regions between 9.5 and 0.5 ppm. The region, containing the residual HOD peak, from 4.7 to 5.0 ppm was excluded from the analysis. Unsupervised multivariate analyses by PCA were done using SIMCA-P (v9.0, Umetrics, Umea, Sweden) employing mean-centered scaling.

Hydrogen peroxide and superoxide staining.

Infected leaf material was collected and incubated for 8 h, either in the presence or absence of 1 mg of 3,3′-DAB per milliliter (D8001; Sigma), dissolved in water (pH 3.8) in the dark, as previously described (Thordal-Christensen et al. 1997). The material was then cleared by boiling three times for 10 min in absolute ethanol. Superoxide detection using NBT staining was performed as described (Adam et al. 1989).

RNA isolation and microarray hybridization.

Total RNA was isolated from freeze-dried leaf tissues infected by *M. graminicola* using the TRIZOL procedure (Invitrogen, San Diego, CA, U.S.A.), following the supplier's protocol and incorporating the suggested additional procedures for polysaccharide-containing tissues. Further purification of the total RNA was achieved by precipitation from a solution of 4 M lithium chloride. Total RNA was used for all microarray and RT-PCR analyses. RNA species were analyzed by agarose gel electrophoresis using morpholinepropanesulfonic acid buffer and formaldehyde.

Labeling of total RNA was by indirect incorporation of reactive AlexaFluor dyes into amine-modified cDNA synthesized using Superscript III reverse transcriptase (SuperScript Indirect cDNA Labeling System, Invitrogen), following the suppliers protocols. 20 μg of total RNA was used in each labeling reaction. AlexaFluor 555 (equivalent to Cy3 dye) was used in the green channel and AlexaFluor 647 (equivalent to Cy5 dye) was used in the red channel. Detailed hybridization and washing conditions were as described at the COGEME website.

A modification to this procedure was applied to increase the stringency and reduce cross-hybridization of homologous plant sequences. This entailed an increase in the temperature of all washing steps to 65°C and the use of a hybridization buffer containing, 50% (vol/vol) Formamide, 5× SSC (1× SSC is 0.15 M NaCl plus 0.015 M sodium citrate) buffer and 0.1% (wt/vol) SDS. The fluorescently labeled slides were scanned using an Axon 4000B scanner with a spot size of 5 μm. Scanning parameters were optimized by preliminary analysis of the output data using GenePix software supplied with the scanner. All subsequent analysis of the data was performed as described by Keon and associates (2005b).

Real-time quantitative PCR.

Genomic DNA was isolated from approximately 100 mg of infected leaf tissue (two 6-cm leaf segments) harvested daily during the infection cycle, using a DNeasy plant mini kit (Qiagen, Hybaid, Cambridge), following the supplier's instructions. Real-time quantitative PCR was performed in order to monitor levels of fungal biomass in infected leaf tissues according to the method of Fraaije and associates (2005), using a Cy5 labeled probe to quantify the presence of the cytochrome *b* gene of *M. graminicola*. DNA (50 ng) was used in a 20-μl PCR reaction. Results were obtained from three replicate timecourse experiments.

Real-time RT-PCR with SYBR-Green detection.

First-strand cDNA was synthesized from total RNA using the SuperScript III first-strand synthesis system for RT-PCR (Invitrogen). Total RNA (5 μg) primed with oligo$(dT)_{20}$ was used in a 20-μl reaction following the suppliers instructions. The resulting cDNA was analyzed using a QuantiTect SYBR Green PCR kit (Qiagen), following the supplier's instructions. cDNA (0.5 μl) was used in a 20-μl PCR reaction, with an annealing temperature of 56°C. Primers were added at a final concentration of 0.25 μM. PCR reactions were run and analyzed using an ABI 7500 real time PCR system, with beta-tubulin acting as the endogenous control. The primers used in the real-time RT-PCR are shown in Table 3.

Microscopy.

Infected leaves stained with DAB and NBT (described above) and unstained controls were fixed in a solution of 10 mM PB buffer plus 3% glutaraldehyde, and then, were dehydrated in an ethanol series, before being embedded in LR White resin. Sections were then cut (1 micron), and the samples were observed using a light microscope Axiophot (Zeiss, Oberkochen, Germany). Images were captured using a DC300 FX digital camera (Leica, Wetzlar, Germany).

Statistics.

The overlap of genes differentially expressed between individual microarray data sets was analyzed as binomial proportion using a generalized linear model with logit LINK (Payne et al. 2005).

ACKNOWLEDGMENTS

We would like to thank G. Kema (PBI, The Netherlands) for the provision of *M. graminicola* isolate IPO323. We thank D. Lovell for help in establishing the leaf-infection bioassay. We gratefully acknowledge the

help of B. Fraaije and H. Cools for real-time PCR analyses and J. Lucas for critical reading of the manuscript. Rothamsted Research receives grant-aided support from the Biotechnology and Biological Sciences Research Council (BBSRC) of the U.K. This study was additionally supported by a BBSRC grant as part of COGEME 1 (34/IGF12505) and the COGEME users fund (BB/C003462/1).

LITERATURE CITED

Adam, A., Farkas, T., Somlyai, G., Hevesi, M., and Kiraly, Z. 1989. Consequence of O_2^- generation during a bacterially induced hyper-sensitive reaction in tobacco: Deterioration of membrane lipids. Physiol. Mol. Plant Pathol. 34:13-26.

Balk, J., and Leaver, C. J. 2001. The PET1-CMS mitochondrial mutation in sunflower is associated with premature programmed cell death and cytochrome c release. Plant Cell 13:1803-1818.

Balk, J., Leaver, C. J., and McCabe, P. F. 1999. Translocation of cytochrome c from the mitochondria to the cytosol occurs during heat-induced programmed cell death in cucumber plants. FEBS (Fed. Eur. Biochem. Soc.) Lett. 463:151-154.

Balk, J., Chew, S. K., Leaver, C. J., and McCabe, P. F. 2003. The intermembrane space of plant mitochondria contains a DNase activity that may be involved in programmed cell death. Plant J. 34:573-583.

Bechtold, U., Karpinski, S., and Mullineaux, P. M. 2005. The influence of the light environment and photosynthesis on oxidative signaling responses in plant-biotrophic pathogen interactions. Plant Cell Environ. 28:1046-1055.

Beers, E. P., and McDowell, J. M. 2001. Regulation and execution of programmed cell death in response to pathogens, stress and developmental cues. Curr. Opin. Plant Biol. 4:561-567.

Beilby, J. P., and Kidby, D. K. 1980. Biochemistry of ungerminated and germinated spores of the vesicular-arbuscular mycorrhizal fungus, *Glomus caledonius*: changes in neutral and polar lipids. J. Lipid Res. 21:739-750.

Boller, T. 1995. Chemoperception of microbial signals in plant cells. Annu. Rev. Plant Physiol. Plant Mol. Biol. 46:189-214.

Both, M., Csukai, M., Strumpf, M. P. H., and Spanu, P. D. 2005. Gene expression profiles of *Blumeria graminis* indicate dynamic changes to primary metabolism during development of an obligate biotrophic pathogen. Plant Cell 17:2107-2122.

Bussink, H.-J., and Oliver, R. P. 2001. Identification of two highly divergent catalase genes in the fungal tomato pathogen, *Cladosporium fulvum*. Eur. J. Biochem 268:15-24.

Calpouzos, L., and Stallknecht, G. F. 1967. Symptoms of cercospora leaf spot of sugar beets influenced by light intensity. Phytopathology 57:799-800.

Chandra-Shekara, A. C., Gupte, M., Navarre, D., Raina, R., Klessig, D., and Kachroo, P. 2006. Light-dependent hypersensitive response and resistance signaling against Turnip crinkle virus in Arabidopsis. Plant J. 45:320-334.

Chichkova, N. V., Kim, S. H., Titova, E. S., Kalkum, M., Morozov, V. S., Rubtsov, Y. P., Kalinina, N. O., Taliansky, M. E., and Vartapetian, A. B. 2004. A plant caspase-like protease activated during the hypersensitive response. Plant Cell 16:157-171.

Coffeen, W. C., and Wolpert, T. J. 2004. Purification and characterisation of serine proteases that exhibit caspase-like activity and are associated with programmed cell death in *Avena sativa*. Plant Cell 16:857-873.

Curtis, M. J., and Wolpert, T. J. 2004. The victorin-induced mitochondrial permeability transition precedes cell shrinkage and biochemical markers of cell death, and shrinkage occurs without loss of membrane integrity. Plant J. 38:244-259.

Daub, M. E., and Ehrenshaft, M. 2000. The photoactivated Cercospora toxin cercosporin: Contributions to plant disease and fundamental biology. Annu. Rev. Phytopathol. 38:461-490.

del Pozo, O., and Lam, E. 1998. Caspases and programmed cell death in the hypersensitive response of plants to pathogens. Curr. Biol. 8:1129-1132.

Duncan, K. E., and Howard, R. J. 2000. Cytological analysis of wheat infection by the leaf blotch pathogen *Mycosphaerella graminicola*. Mycol. Res. 104:1074-1082.

Eyal, Z. 1999. The *Septoria tritici* and *Stagonospora nodorum* blotch diseases of wheat. Eur. J. Plant Path. 105:629-641.

Fraaije, B. A., Cools, H. J., Fountaine, J., Lovell, D. J., Motteram, J., West, J. S., and Lucas, J. A. 2005. Role of ascospores in further spread of QoI-resistant cytochrome b alleles (G143A) in field populations of *Mycosphaerella graminicola*. Phytopathology 95:933-941.

Glazebrook, J. 2005. Contrasting mechanisms of defense against biotrophic and necrotrophic pathogens. Annu. Rev. Phytopathol. 43:205-227.

Goodwin, S. B. 2004. Minimum phylogenetic coverage: An additional criterion to guide the selection of microbial pathogens for initial genomic sequencing efforts. Phytopathology 94:800-804.

Goodwin, P. H., Li, J. R., and Jin, S. M. 2001. A catalase gene of *Colletotrichum gloeosporioides* f. sp *malvae* is highly expressed during the necrotrophic phase of infection of round-leaved mallow, Malva pusilla. FEMS (Fed. Eur. Microbiol. Soc.) Microbiol. Lett. 202:103-107.

Govrin, E. M., and Levine, A. 2000. The hypersensitive response facilitates plant infection by the necrotrophic pathogen *Botrytis cinerea*. Curr. Biol. 10:751-757.

Greenberg, J. T., and Yao, N. 2004. The role and regulation of programmed cell death in plant-pathogen interactions. Cell. Microbiol. 6:201-211.

Hammond-Kosack, K. E., and Jones, J. D. G. 1996. Resistance gene-dependent plant defence responses. Plant Cell 8:1773-1791.

Hatsugai, N., Kuroyanagi, M., Yamada, K., Meshi, T., Tsuda, S., Kondo, M., Nishimura, M., and Hara-Nishimura, I. 2004. A plant vacuolar protease, VPE, mediates virus-induced hypersensitive cell death. Science 305:855-858.

Heath, M. C. 2000. Hypersensitive response-related death. Plant Mol. Biol. 44:321-334.

Hisada, H., Hata, Y., Kawato, A., Abe, Y., and Akita, O. 2005. Cloning and expression analysis of two catalase genes from *Aspergillus oryzae*. J. Bacteriol.:562-568.

Huckelhoven, R., Dechert, C., and Kogel, K. H. 2003. Overexpression of barley BAX inhibitor 1 induces breakdown of mlo-mediated penetration resistance to *Blumeria graminis*. Proc. Natl. Acad. Sci. U.S.A. 100:5555-5560.

Jones, A. 2000. Does the plant mitochondrion integrate cellular stress and regulate programmed cell death? Trends Plant Sci. 5:225-230.

Karpinski, S., Gabrys, H., Mateo, A., Karpinska, B., and Mullineaux, P. M. 2003. Light perception in plant disease defence signaling. Curr. Opin. Plant Biol. 6:390-396.

Kema, G. H. J., Yu, D. Z., Rijkenberg, F. H. J., Shaw, M. W., and Baayen, R. P. 1996. Histology of the pathogenesis of *Mycosphaerella graminicola* in wheat. Phytopathology 86:777-786.

Keon, J., Antoniw, J., Rudd, J. J., Skinner, W., Hargreaves, J., and Hammond-Kosack, K. E. 2005a. Analysis of expressed sequence tags from the wheat leaf blotch pathogen *Mycosphaerella graminicola* (anamorph *Septoria tritici*). Fungal Genet. Biol. 42:376-389.

Keon, J., Rudd, J. J., Antoniw, J., Skinner, W., Hargreaves, J., and Hammond-Kosack, K. E. 2005b. Metabolic and stress adaptation by *Mycosphaerella graminicola* during sporulation in its host revealed through microarray transcription profiling. Mol. Plant Pathol. 6:527-540.

Krause, M., and Durner, J. 2004. Harpin inactivates mitochondria in *Arabidopsis* suspension cells. Mol. Plant-Microbe Interact. 17:131-139.

Lara-Ortiz, T., Riveros-Rosas, H., and Aguirre, J. 2003. Reactive oxygen species generated by microbial NADPH oxidase NoxA regulate sexual development in *Aspergillus nidulans*. Mol. Microbiol. 50:1241-1255.

Lincoln, J. E., Richael, C., Overduin, B., Smith, K., Bostock, R., and Gilchrist, D. G. 2002. Expression of the antiapoptotic baculvirus p35 gene in tomato blocks programmed cell death and provides broad-spectrum resistance to disease. Proc. Natl. Acad. Sci. U.S.A. 99:15217-15221.

Liu, Y., Schiff, M., Czymmek, K., Talloczy, Z., Levine, B., and Dinesh-Kumar, S. P. 2005. Autophagy regulates programmed cell death during the plant innate immune response. Cell 121:567-577.

Luttrell, E. S. 1974. Parasitism of fungi on vascular plants. Mycologia 66:1-15.

Malagnac, F., Lalucque, H., Lepere, G., and Silar, P. 2004. Two NADPH oxidase isoforms are required for sexual reproduction and ascospore germination in the filamentous fungus *Podospora anserina*. Fungal Genet. Biol. 41:982-997.

Manning, V. A., and Ciuffetti, L. M. 2005. Localization of Ptr ToxA produced by *Pyrenophora tritici-repentis* reveals protein import into wheat mesophyll cells. Plant Cell 17:3203-3212.

Montillet, J. L., Chamnongpol, S., Rusterucci, C., Dat, J., van de Cotte, B., Agnel, J. P., Battesti, C., Inze, D., Van Breusegem, F., and Triantaphylides, C. 2005. Fatty acid hydroperoxides and H_2O_2 in the execution of hypersensitive cell death in tobacco leaves. Plant Physiol. 138:1516-1526.

Nagata, S., Nagase, H., Kawane, K., Mukae, N., and Fukuyama, H. 2003. Degradation of chromosomal DNA during apoptosis. Cell Death Differ. 10:108-116.

Navarre, D. A., and Wolpert, T. J. 1999a. Effects of light and CO_2 on victorin-induced symptom development in oats. Physiol. Mol. Plant Pathol. 55:237-242.

Navarre, D. A., and Wolpert, T. J. 1999b. Victorin induction of an apoptotic/senescence-like response in oats. Plant Cell 11:237-249.

Nurnberger, T., and Lipka, V. 2005. Non-host resistance in plants: new insights into an old phenomenon. Mol. Plant Pathol. 6:335-345.

Oliver, R. P., and Ipcho, S. V. S. 2004. Arabidopsis pathology breathes new life into the necrotrophs-vs.-biotrophs classification of fungal pathogens. Mol. Plant Pathol. 5:347-352.

Parbery, D. G. 1996. Trophism and the ecology of fungi associated with plants. Biol. Rev.:473-527.

Payne, R. W., Harding, S. A., Murray, D. A., Soutar, D. M., Baird, D. B., Welham, S. J., Kane, A. F., Gilmour, A. R., Thompson, R., Webster, R., and Tunnicliffe Wilson, G. 2005. The Guide to GenStat Release 8, Part 2: Statistics. VSN International, Oxford.

Perfect, S. E., O'Connell, R. J., Green, E. F., Doering-Saad, C., and Green, J. R. 1998. Expression cloning of a fungal proline-rich glycoprotein specific to the biotrophic interface formed in the *Colletotrichum*-bean interaction. Plant J. 15:273-279.

Ravagnan, L., Roumier, T., and Kroemer, G. 2002. Mitochondria, the killer organelles and their weapons. J. Cell. Physiol. 192:131-137.

Rotem, J., Wendt, U., and Kranz, J. 1988. The effect of sunlight on symptom expression of *Alternaria alternata* on cotton. Plant Pathol. 37:12-15.

Ryerson, D. E., and Heath, M. C. 1996. Cleavage of nuclear DNA into oligonucleosomal fragments during cell death induced by fungal infection or by abiotic treatments. Plant Cell 8:393-402.

Shetty, N. P., Kristensen, B. K., Newman, M. A., Møller, K., Gregersen, P. L., and Jørgensen, H. J. L. 2003. Association of hydrogen peroxide with restriction of *Septoria tritici* in resistant wheat. Physiol. Mol. Plant Pathol. 62:333-346.

Solomon, P. S., and Oliver, R. P. 2001. The nitrogen content of the tomato leaf apoplast increases during infection by *Cladosporium fulvum*. Planta 213:241-249.

Solomon, P. S., Lee, R. C., Wilson, T. J., and Oliver, R. P. 2004. Pathogenicity of *Stagonospora nodorum* requires malate synthase. Mol. Microbiol. 53:1065-1073.

Stone, J. M., Heard, J. E., Asai, T., and Ausubel, F. M. 2000. Stimulation of fungal-mediated cell death by fumonisin B1 and selection of fumonisin B1-resistant (*fbr*) arabidopsis mutants. Plant Cell 12:1811-1822.

Talbot, N. J., McCafferty, H. R. K., Ma, M., Moore, K., and Hamer, J. E. 1997. Nitrogen starvation of the rice blast fungus *Magnaporthe grisea* may act as an environmental cue for disease symptom expression. Physiol. Mol. Plant Pathol. 50:179-195.

Thordal-Christensen, H., Zhang, Z., Wei, Y., and Collinge, D. B. 1997. Subcellular localization of H_2O_2 in plants. H_2O_2 accumulation in papillae and hypersensitive response during the barley-powdery mildew interaction. Plant J. 11:1187-1194.

Thrower, L. B. 1966. Terminology for plant parasites. Phytopathol. Zeit. 56:258-259.

Tiwari, B. S., Belenghi, B., and Levine, A. 2002. Oxidative stress increased respiration and generation of reactive oxygen species, resulting in ATP depletion, opening of mitochondrial permeability transition, and programmed cell death. Plant Physiol. 128:1271-1281.

Todd, R. B., Murphy, R. L., Martin, H. M., Sharp, J. A., Davis, M. A., Katz, M. E., and Hynes, M. J. 1997. The acetate regulatory gene *facB* of *Aspergillus nidulans* encodes a $Zn(II)_2Cys_6$ transcriptional activator. Mol. Gen. Genet. 254:495-504.

Van Baarlen, P., Staats, M., and Van Kan, J. A. L. 2004. Induction of programmed cell death in lily by the fungal pathogen *Botrytis elliptica*. Mol. Plant Pathol. 5:559-574.

Van den Ackerveken, G., Dunn, R., Cozijnsen, A., Vossen, J., van den Broek, H., and de Wit, P. 1994. Nitrogen limitation induces expression of the avirulence gene *avr9* in the tomato pathogen *Cladosporium fulvum*. Mol. Gen. Genet. 243:277-285.

Van Doorn, W. G., and Woltering, E. J. 2005. Many ways to exit? Cell death categories in plants. Trends Plant Sci. 10:117-122.

Woltering, E. J. 2004. Death proteases come alive. Trends Plant Sci. 9:469-472.

Yao, N., Imai, S., Tada, Y., Nakayashiki, H., Tosa, Y., Park, P., and Mayama, S. 2002. Apoptotic cell death is a common response to pathogen attack in oats. Mol. Plant-Microbe Interact. 15:1000-1007.

Yao, N., Eisfelder, B. J., Marvin, J., and Greenberg, J. T. 2004. The mitochondrion—An organelle commonly involved in programmed cell death in *Arabidopsis thaliana*. Plant J. 40:596-610.

Zuppini, A., Navazio, L., Sella, L., Castiglioni, J., Favaron, F., and Mariani, P. 2005. An endopolygalacturonase from Sclerotinia sclerotiorum induces calcium-mediated signaling and programmed cell death in soybean cells. Mol. Plant-Microbe Interact. 18:849-855.

AUTHOR-RECOMMENDED INTERNET RESOURCE

COGEME (Consortioum for the Functional Genomics of Microbial Eukaryotes) website:
www.cogeme.man.ac.uk/Facilities/TRF%20Protocols.htm